American Mineralogist, Volume 58, pages 451–456, 1973

The Polarized Spectra of Iron in Silicates. II. Olivine

W. ALAN RUNCIMAN, DIPANKAR SENGUPTA, AND J. TERRY GOURLEY

Department of Solid State Physics, Research School of Physical Sciences, The Australian National University, Canberra, A.C.T., 2600, Australia

Abstract

The interpretation of the polarized absorption spectra of ferrous iron in olivine (Burns, 1970a, b) has been based on pseudo-trigonal symmetry of the $M(2)$ sites and pseudo-tetragonal symmetry of the $M(1)$ sites. This analysis is shown to be faulty, and an alternative explanation is provided which is based on C_{2v} symmetry. Polarized spectra have been obtained of an olivine crystal at room and liquid helium temperatures covering the infrared, visible, and ultraviolet ranges from 200–45000 cm^{-1}. Energy levels are calculated on a model which extends that used for enstatite in Part I (Runciman, Sengupta, and Marshall, 1973). The intensity ratios observed are discussed on the basis of mixing of the states involved with the lowest charge transfer state.

Introduction

Polarized spectra of olivine (peridot) have been previously reported by Farrell and Newnham (1965), Grum-Grzhimailo, Boksha, and Varina (1969), Shankland (1969), and Burns (1970, a,b). The distinctive feature is a very strong γ band at 9540 cm^{-1}. The visible and near infrared ranges have been examined with unpolarized radiation by Clark (1957) and by White and Keester (1966). The vibrational spectrum in the range 200–4000 cm^{-1} has been investigated (Duke and Stephens, 1964; Burns and Huggins, 1972). The method of analysis of the spectrum is an extension of that used for enstatite (Runciman, Sengupta, and Marshall, 1973) which will be referred to as Part I.

Absorption Spectra of Olivine

The experimental technique was similar to that described in Part I. The crystal examined was a piece of uncut peridot, the gem name for the mineral olivine. Olivine has the formula $(Mg,Fe)_2SiO_4$ and varies from forsterite, Mg_2SiO_4 to fayalite, Fe_2SiO_4. The present sample, probably from Burma, was found by electron microprobe analysis to contain in wt percent: SiO_2, 40.68; MnO, 0.11; CaO, 0.04; FeO, 9.97; MgO, 49.22; NiO, 0.36. In terms of the corresponding silicates it contains in mole percent: 89.2, Mg_2SiO_4; 10.2, Fe_2SiO_4; 0.4, Ni_2SiO_4; 0.1, Mn_2SiO_4; 0.1, Ca_2SiO_4. A block was cut with dimensions 5.00 × 3.24 × 3.24 mm oriented along the α, β and γ axes. Polarized spectra were obtained, and are shown normalized to a thickness of 1 mm in Figure 1. For ranges of higher absorption, crystals of 100 μm thickness were used. An important feature of the results is the crossover of the polarization spectra near 37000 cm^{-1} (Fig. 2) as this indicates that the intense charge transfer band is predominantly γ polarized, and not β as suggested by Burns (1970a) on the basis of spectra extending up to 25000 cm^{-1}. Spectra of the crystals at liquid helium temperature are shown in Figures 3–5 and show considerably more detail, but no striking new features. The main features are still the γ polarized band at 9540 cm^{-1}, with a prominent shoulder on the low energy side, and the intense infrared bands in the range 1500–2100 cm^{-1}.

The far-infrared region of the spectrum 180–1200 cm^{-1} was obtained using powdered sample in a CsI disc. The spectra at room temperature and liquid helium temperature are shown in Figure 6. The band positions and intensities are consistent with the spectra of Duke and Stephens (1964) and Burns and Huggins (1972). A number of very weak bands have been observed around the 3500 cm^{-1} region. These bands are possibly due to the presence of traces of OH in the lattice.

Crystal Structure

Olivine has an orthorhombic crystal structure with space group *Pnma* (No. 62) and contains 4 molecules in the unit cell, a_o = 4.77Å, b_o = 10.26Å, c_o = 6.00Å. The crystal and optic axes are related by $\alpha = b$, $\beta = c$, $\gamma = a$. The crystal structure has been studied by Hanke (1965) and is based on a

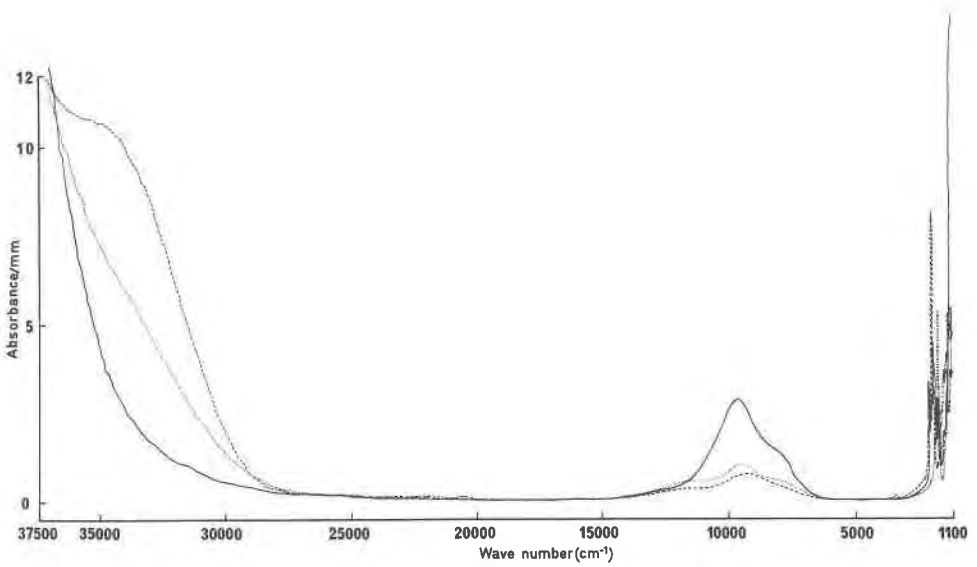

FIG. 1. Room temperature spectrum of olivine ···· α spectrum, --- β spectrum, ——— γ spectrum.

hexagonal close packed array of oxygen atoms with silicon atoms in the tetrahedral positions and magnesium atoms on two octahedral sites, $M(1)$ and $M(2)$. $M(1)$ is a $(4a)$ site of C_i (i) symmetry and $M(2)$ is a $(4c)$ site of $C_s(m)$ symmetry. A Mössbauer investigation of olivines by Bush, Hafner, and Virgo (1970) indicates only slight preferential distribution among the sites. Burns (1970a) has presented arguments on the basis of optical data for a slight preference of ferrous iron for $M(2)$ sites. Transition probabilities are usually an order of magnitude smaller for centrosymmetric sites. Hence, contrary to the interpretation of the spectra given by Grum-Grzhimailo, Boksha, and Varina (1969), an explanation for the major features of the spectra will be sought in terms of $M(2)$ ferrous ions.

The projection of the $M(2)$ site with nearest

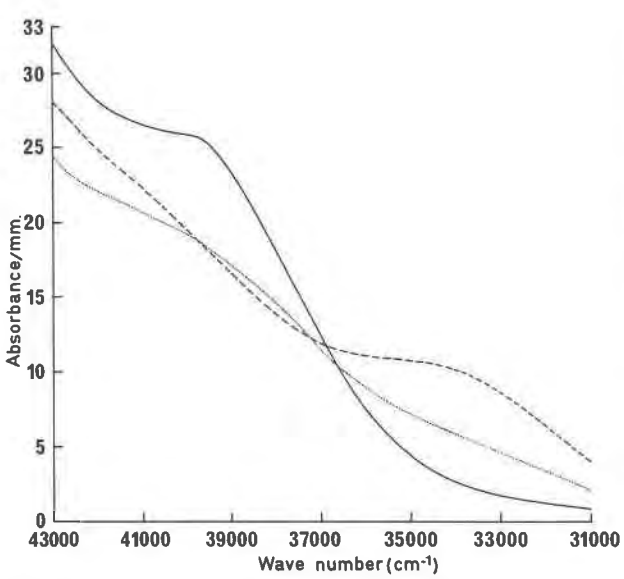

FIG. 2. 31000-43000 cm^{-1} room temperature spectrum of olivine ···· α spectrum, - - - β spectrum, —— γ spectrum.

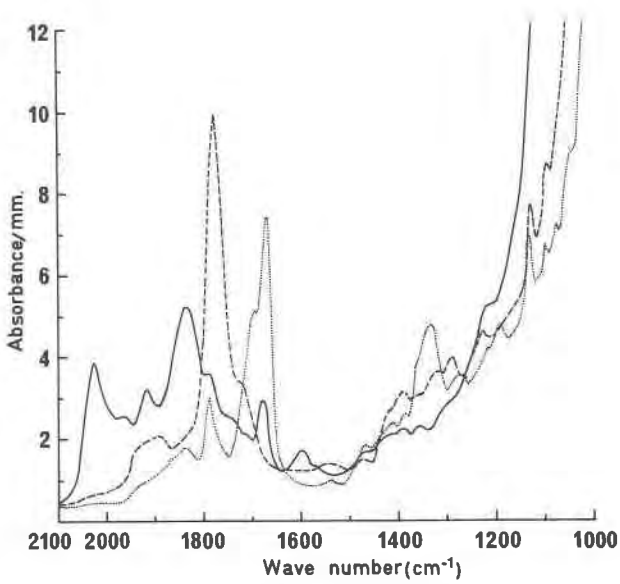

FIG. 3. 1000 cm^{-1} to 2100 cm^{-1} helium temperature spectrum of olivine ···· α spectrum, - - - β spectrum, —— γ spectrum.

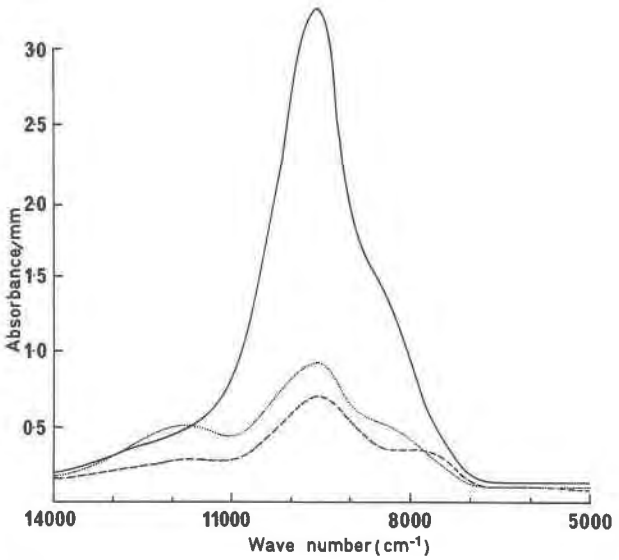

FIG. 4. 5000–14000 cm^{-1} helium temperature spectrum of olivine ···· α spectrum, - - - β spectrum, —— γ spectrum.

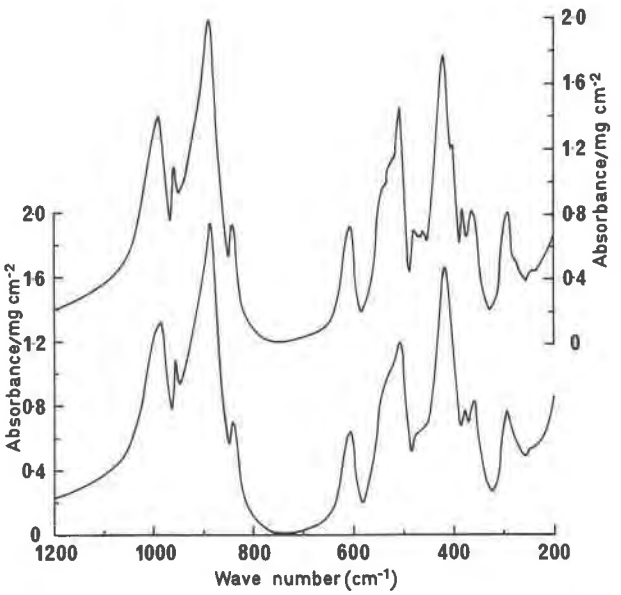

FIG. 6. 200–1200 cm^{-1} spectra of olivine in a CsI disc. Upper section at helium temperature, lower section at room temperature.

neighbor oxygen atoms in the α-γ plane is shown in Figure 7. This is the mirror plane of the crystal, and O(1) and O(2) atoms lie in the plane. The four O(3) atoms are also shown and their distances along the β axis are indicated. Burns (1970 a,b) has regarded the site as having a trigonal distortion. However the major distortion is due to a next nearest neighbor silicon atom which elongates two M(2)-O(3) bonds and distorts the angles (Fig. 7). Hence the distortion is much better described as C_{2v} whereas the exact symmetry is C_s, which is too low a symmetry to be very helpful in a crystal field analysis. The two-fold axis of pseudo-C_{2v} symmetry must lie in the α-γ mirror plane and is shown (Fig. 7) as the Z axis. The angle between Z and the γ axis, which is normal to the hexagonal close packed layers of oxygen atoms, is taken to be $\cos^{-1}(2/3)^{1/2}$, or about 35°. The axis normal to Z in the α-γ plane is shown as Y. This axis is close to the original fourfold axis O(2)-M(2)-O(1). This is also a direction of

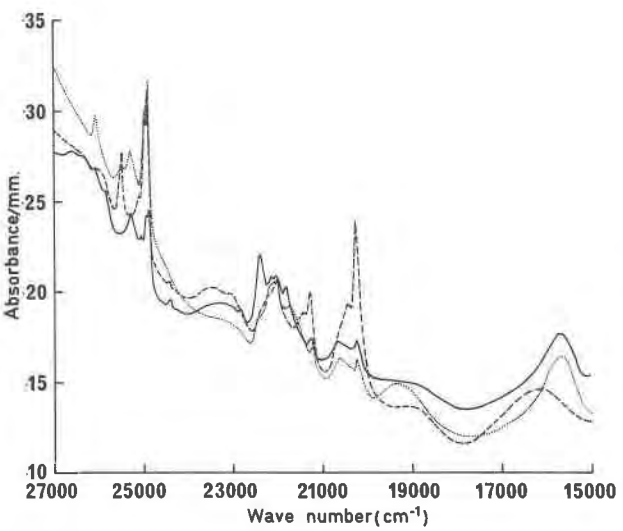

FIG. 5. 15000–27000 cm^{-1} helium temperature spectrum of olivine ···· α spectrum, - - - β spectrum, —— γ spectrum.

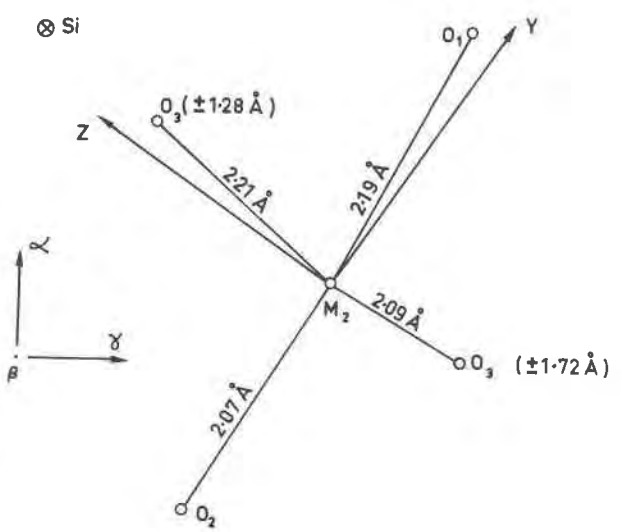

FIG. 7. Projection of the M(2) site on the mirror plane.

strong distortion as pointed out by Hanke (1965). This distortion can best be described as an asymmetric displacement of the metal ion along this axis.

Infrared Spectrum

The main features of the infrared spectrum are shown in Figures 3 and 6. The positions and intensities of the main bands are listed in Table 1. The bands in the 1100–2000 cm^{-1} region can be identified as combinations of the fundamental modes as indicated in Table 1. The spectrum of synthetic forsterite has also been measured and found to be the same as for the peridot crystal in the 180–1200 cm^{-1} region (Fig. 6). Only the α- and β-polarized spectra have been studied in the 2100–1000 cm^{-1} region. The important difference of this spectrum from that in Figure 3 is the absence of the strong 1668 cm^{-1} (α-polarized) and 1775 cm^{-1} (β-polarized) bands. These bands are therefore attributed to the ferrous iron present in olivine. The 1668 cm^{-1} band has been assigned to the $A_1 \rightarrow B_2$ electronic transition. The origin of the 1775 cm^{-1} band is not clear.

Crystal Field Analysis

The failure of the trigonal field approach is best illustrated by the 9540 cm^{-1} band. Burns (1970a) attributes this band to an $A \rightarrow E$ transition in C_{3v} symmetry. In this case it would have α and β components and no γ, whereas it is dominantly γ polarized. An analysis was therefore attempted with C_{2v} symmetry as in Part I. Neglecting spin-orbit interaction, the only way of explaining the strong γ band, using the selection rules and wave functions in Tables 2 and 3 of Part I, is to assign both the ground state and the state with energy 9540 cm^{-1} to wave functions of A_1 symmetry. The other ^5E state at 9100 cm^{-1} has B_1 symmetry. The infrared band at 1668 cm^{-1} is assigned to the B_2 component of the $^5T_2$ ground state. Such a small splitting of the ^5E state leads to difficulties as A_1 ceases to be the ground state. However, as noted in the discussion of crystal structure, there is a large distortion along the Y axis, which gives rise to a B_4^0 term with the Y axis for quantization. Since in D_{4h} symmetry all the terms have different symmetry states, this leads to no new off-diagonal terms. The treatment of this term has been used as an example by Sugano, Tanabe, and Kamimura (1970). The added terms to the diagonal elements are $6\delta_3$ for A_1, δ_3 for B_1 (^5E); $-4\delta_3$ for B_2, $-4\delta_3$ for A_2 and δ_3 for A_1 ($^5T_2$), where $\delta_3 = B_4^0/21$ referred to the Y axis.

Since the A_2 level is not identified, there is uncertainty in the values of parameters. Assuming the A_2 level to be located at 300 cm^{-1}, the following parameter values are deduced (in cm^{-1}).

$$\Delta = 8950, \delta_1 = 244, \delta_2 = 570, \delta_3 = -68.$$

It is unlikely that the A_2 level is lower than 300 cm^{-1}; otherwise marked changes would be expected on lowering the temperature from room temperature to liquid helium temperature. Since no major effects are seen, but only an increase in the resolution of the bands, this is a lower limit for A_2 and hence an upper limit for δ_3, which is negative.

Spin-orbit Splitting

The spin-orbit splittings of the $^5T_2$ and ^5E levels were calculated using the method described in Part I. The results are shown in Table 2 for a spin-orbit splitting parameter of 400 cm^{-1}.

For the upper $^5A_1$, $^5B_1$ states and also for the $^5B_2$ state, the splitting is essentially quenched. However, there is a rather large splitting of the ground state. At room temperature it is reasonable to assume that all the spin-orbit levels are more or less equally occupied. At low temperatures only the $\tilde{A}_1$ and B_2 spin-orbit states of the ground multiplet are significantly populated. The liquid helium temperature spectra (Fig. 4) show maxima in all polarizations at 9540 cm^{-1}, whereas there was a 400 cm^{-1} splitting at room temperature (Fig. 1).

Compared to enstatite, the visible spectrum for olivine shows more structure. However, once again, due to the spin-orbit splitting and the low symmetry crystal field, the energy levels due to different multiplets overlap. The two broad bands at about 15800 cm^{-1} and 19000 cm^{-1} can be assigned to $^3T_1$ and $^3T_2$ transitions respectively.

TABLE 1. Infrared Absorption Bands

CsI Disc		100μ thick sample			
Position (cm^{-1})	Intensity (Arbitrary)	Position (cm^{-1})	Intensity Abs/mm	Polarization	Assignment
290	0.68	1124	-	α,β	506 + 610
360	0.66	1330	-	α	890 + 420
380	0.62	1668	5.25	α	840 + 840
420	1.22	1676	2.8	γ	
506	0.90	1775	8.0	β	888 + 888
		1786	3.5(2.75)	γ(α)	
610	0.52	1840	4.5	γ	
840	0.57	1920	3.0	γ	955 + 955
888	1.30	2028	3.3	γ	990 + 990
955	0.82				
990	0.98				

Polarization Intensities

Since the plane normal to the β axis is a mirror plane, the β spectrum should be different from the α and γ spectra. Using the orientations of the X, Y, Z axes previously defined in the section on crystal structure, the relative intensities in the X, Y, and Z transitions are calculated to be as follows:

	α	β	γ
X	0	1	0
Y	0.67	0	0.33
Z	0.33	0	0.67

This explains the Z intensity at 9540 cm^{-1} and the X band at 9100 cm^{-1} reasonably well, but it fails to explain the shoulders in all spectra at 8100 cm^{-1} or shoulders in the α and β spectra at 11700 cm^{-1} (Fig. 4). Finally, there is, as expected, a strong Y band with approximately a 2:1 ratio of α:γ intensities at 1668 cm^{-1}.

The possible origin of the shoulders in all spectra at 8100 cm^{-1} in the α and β spectra at 11700 cm^{-1} is now considered. Burns (1970a) assigned the 9100 cm^{-1} and 11700 cm^{-1} bands to Fe^{2+} ions on $M(1)$ sites and has calculated the ratio of intensity of these bands to the central 9540 cm^{-1} band to be 0.60. As stated previously, ferrous ions are about equally distributed among the $M(1)$ and $M(2)$ sites. However the $M(1)$ site is centrosymmetric, and electric dipole transitions are forbidden between levels belonging to the same configuration. The only way these transitions can gain intensity is through vibronic coupling. To test this possibility, the temperature dependence of the bands was studied over the temperature range 4 K to 300 K. Within experimental error, no temperature dependence of the bands was detected. Vibronic coupling in the ground state gives the well-known coth ($\hbar\omega/2kT$) temperature dependence, where ω is the average frequency of the lattice modes. Absence of temperature dependence goes against the notion that strong vibronic coupling is required to produce the desired intensity ratio. Thus it appears that there is no simple explanation for the prominent shoulders in the olivine spectra.

Point Charge Calculations

The intensity calculations depend on odd crystal field terms, which do not emerge from an energy level analysis. Therefore, despite the recognized limitations of the method, these were calculated using a point charge model. The atomic positions were taken from Hanke (1965). The lattice sum was calculated using a variation of the chargeless cluster method developed by Sengupta and Artman (1970) who cite earlier references. It was assumed that Si, Mg and O sites had +4, +2 and −2 units of charge respectively. The lattice sum results are shown in the first and third columns of Table 3. The crystal fields are calculated using $\langle r \rangle = 0.5536$Å and $\langle r^3 \rangle = 0.3393(\text{Å})^3$, as obtained from the Fe^{2+} Hartree-Fock wave functions of Watson (1959). It is obvious from the calculation that crystal fields of T_{2u} symmetry type are very small compared to T_{1u} crystal fields. Experimentally the

TABLE 2. Spin-Orbit Splittings of ^5D Energy Levels

Experimental (cm^{-1})			Theoretical (cm^{-1})		
Designation	at 4.2 K	at 295 K	Designation	Position	Centre of gravity
			A_1	9638	
			B_2	9637	
$^5A_1$	9540	9540	A_2	9632	9632
			B_1	9625	
			A_1	9625	
			B_1	9190	
			A_1	9190	
$^5B_1$	9540	9100	B_2	9182	9185
			A_2	9182	
			B_1	9180	
			B_2	1696	
			B_2	1695	
$^5B_2$	1668	1668	A_1	1674	1681
			B_1	1673	
			A_2	1666	
			A_1	497	
			B_1	497	
$^5A_2$	-	-	B_1	392	422
			A_2	388	
			B_2	336	
			A_1	136	
			B_1	98	
$^5A_1$	-	-	A_2	78	62
			A_1	0.27	
			B_2	0	

TABLE 3. Point Charge Calculation of Odd Crystal Fields

Symmetry Type	1st Order		3rd Order	
	Lattice Sum ($\lvert e\rvert/\text{Å}^2$)	Crystal Field (cm^{-1})	Lattice Sum ($\lvert e\rvert/\text{Å}^4$)	Crystal Field (cm^{-1})
T_{1uX}	0	0	0	0
T_{1uY}	-0.1177	-3702	-0.1093	-3213
T_{1uZ}	0.0317	989	-0.1390	-4086
T_{2uX}			-0.00231	-68
T_{2uY}			0	0
T_{2uZ}			0	0

Z and X intensities are about 4 to 1. Table 6 of Part I seems to indicate that for olivine a T_{2uX} charge transfer state coupled with a T_{1uZ} crystal field provides the dominant mechanism for band intensities. The zero results for T_{1uX}, T_{2uY}, and T_{2uZ} are due to the symmetry plane and provided a useful check on the computer calculation. The large T_{1uY} crystal field terms indicate that the site symmetry is appreciably different from C_{2v}, as these terms are zero for such symmetry. Physically these terms result from the distortion in the Y direction noted by Hanke (1965). The crystal field values calculated on the point charge model cannot be used for exact intensity calculations, since the crystallographic results show that there is considerable covalent bonding in the SiO_4 tetrahedra.

Conclusions

In this paper and in Part I it has been shown that the absorption spectrum of ferrous iron in enstatite and olivine is best considered in terms of C_{2v} symmetry. This model is applicable in many other cases including the diopside-hedenbergite series and the cummingtonite-grunerite series discussed by Burns (1970b) who gives many references to earlier work. Indeed some of these minerals have ferrous ions in sites of C_{2v} symmetry, or more closely approximating to it than the minerals enstatite and olivine. It is important that the theoretical basis for the absorption spectrum be put on a firm basis before conclusions are drawn concerning site population and the enrichment of transition metal ions in certain minerals. It seems likely that the details of the model proposed could best be tested in the low energy region using microwave and far infrared techniques to establish the energies and states of the low lying levels.

Acknowledgments

The assistance is acknowledged of the Department of Geophysics and Geochemistry, Australian National University, in carrying out the electron microprobe analysis of both the enstatite and olivine samples. Dr. A. Duba kindly supplied the synthetic forsterite crystals. We are also grateful to Dr. J. Ferguson of the Research School of Chemistry for introducing us to the flow-tube technique used for the helium temperature experiments on the Cary 17 spectrophotometer.

References

Burns, R. G. (1970a) Crystal field spectra and evidence of cation ordering in olivine minerals. *Amer. Mineral.* **55,** 1608–1632.

——— (1970b) *Mineralogical Applications of Crystal Field Theory*. Cambridge University Press.

———, and F. E. Huggins (1972) Cation determinative curves for Mg-Fe-Mn olivines from vibrational spectra. *Amer. Mineral.* **57,** 967–985.

Bush, W. R., S. S. Hafner, and D. Virgo (1970) Some ordering of iron and magnesium at the octahedrally coordinated sites in a magnesium-rich olivine. *Nature,* **227,** 1339–1341.

Clark, S. P. (1957) Absorption spectra of some silicates in the visible and near infrared. *Amer. Mineral.* **42,** 732–742.

Duke, D. A., and J. D. Stephens (1964) Infrared investigation of the olivine group minerals. *Amer. Mineral.* **49,** 1388–1406.

Farrell, E. F., and R. E. Newnham (1965) Crystal-field spectra of chrysoberyl, alexandrite, peridot, and sinhalite. *Amer. Mineral.* **50,** 1972–1981.

Grum-Grzhimailo, S. V., O. N. Boksha, and T. M. Varina (1969) The absorption spectrum of olivine. *Sov. Phys. Crystallogr.* **14,** 272–274.

Hanke, K. (1965) Beiträge zu kristallstrukturen vom olivin-typ. *Beitr. Mineral. Petrog.* **11,** 535–558.

Runciman, W. A., D. Sengupta, and M. Marshall (1973) The polarized spectra of iron in silicates. I. Enstatite. *Amer. Mineral.* **58,** 444–450.

Sengupta, D., and J. O. Artman (1970) Crystal field shielding parameters for Nd^{3+} and Np^{4+}. *Phys. Rev.* **B1,** 2986–2988.

Shankland, T. J. (1969) Transport properties of olivines. *In,* S. K. Runcorn, ed., The Application of Modern Physics in the Earth and Planetary Interiors. John Wiley and Sons, New York.

Sugano, S., Y. Tanabe, and H. Kamimura (1970) *Multiplets of Transition-metal Ions in Crystals.* Academic Press, New York.

Watson, R. E. (1959) Iron Series Hartree-Fock Calculations, *MIT Solid State Physics, Tech. Report No.* **12.**

White, W. B., and K. L. Keester (1966) Optical absorption spectra of iron in the rock-forming silicates. *Amer. Mineral.* **51,** 774–791.

Manuscript received, July 17, 1972; accepted for publication, December 27, 1972